Hydrogen-induced structural change in $Ni_{90}Al_{10}$ metallic glass

Kyoung-Won Park[a], Yoji Shibutani[b], Eric Fleury[a,*]

[a] High Temperature Energy Materials Center, Korea Institute of Science and Technology, Seoul 136-791, Republic of Korea
[b] Department of Mechanical Engineering, Osaka University, Osaka 565-0871, Japan

ARTICLE INFO

ABSTRACT

$Ni_{90}Al_{10}$ amorphous membranes were prepared by means of molecular dynamics (MD) simulation technique with the aim of investigating the structural evolution induced by hydrogen with respect to hydrogen concentration. The short-range ordered (SRO) structures of the as-cast model sample and the structural change by hydrogen charging were analyzed using Voronoi tessellation method. This study indicates that prism and prism-like structures with low coordination number are generated, while intrinsically stable SRO structures in the amorphous membrane annihilate upon hydrogen charging. We discussed the relationship between these local atomic changes and the structural stability which was evaluated from the potential energy change point of view.

© 2011 Elsevier B.V. All rights reserved.

1. Introduction

Metallic glasses with functional properties have recently been at the center of attention in the field of hydrogen separable membrane. The reason for this interest is the superior resistance to hydrogen embrittlement of the hydrogen separable amorphous membranes in comparison to the crystallized one [1]. However, as a membrane material for hydrogen separation, not only the mechanical strength but also the permeability and catalytic activity of the surface for the dissociation of hydrogen molecules into atoms [2] should be satisfied [1]. So far, thin Pd coating layers have been generally used as catalyst to activate hydrogen molecules, although a few studies have been focused on the development of alternative catalyst materials [2,3]. Therefore, many efforts have been devoted to improve the hydrogen permeability of alloys by focusing on developing new chemical composition of amorphous alloys [4–7]. Due to their endeavor, values of hydrogen permeability for Ni-based amorphous ribbons comparing to those of Pd-alloys could be obtained [8,9].

Although values of hydrogen permeability are sufficient for commercial use, the main difficulty in the long term application of metal membranes is the hydrogen embrittlement [1], which is a common feature in most metals operating in hydrogen atmosphere. Accordingly, many researchers have studied the change in the mechanical properties by hydrogenation in order to enhance the resistance to hydrogen embrittlement of alloys [10–14]. Despite these extensive studies, change in the local atomic structures induced by hydrogen charging and its correlation with the embrittlement occurring during hydrogen permeation have remained unclear. Therefore, in this study, the structural change of amorphous membrane by hydrogen charging was examined by molecular dynamic (MD) simulation technique for a $Ni_{90}Al_{10}$ model alloy. The evolution of the local atomic structures occurring by hydrogenation was analyzed in order to find a strategy to improve the hydrogen permeation properties.

2. Materials and methods

Molecular dynamics simulation is a very useful tool in materials research to provide an atomic description of the structural change in the hydrogenated sample. Using this tool, $Ni_{90}Al_{10}$ model sample (7.355 nm × 18.145 nm × 4.037 nm) was prepared by employing Ni–Al–H EAM (Embedded Atom Method) potential [15,16] and applying periodic boundary conditions to 3-dimensional (3D) directions in order to more closely describe real structures of membrane and to eliminate surface effects. In $Ni_{90}Al_{10}$ parallelepiped samples, Ni and Al atoms (totally 32,000) are randomly positioned at simulation cell of FCC and then heated to 4000 K. After sufficient relaxation until the energy saturates, the samples were cooled to 50 K at a rate of 10^{13} K/s by keeping the external pressure along the three directions at zero pressure using the constant-pressure and constant-temperature NPT (constant number of atoms, pressure, temperature) ensemble. The cooled samples were again sufficiently relaxed at 50 K.

Experimentally, in order to investigate the hydrogen embrittlement, electrocharging method is frequently used [14]. This is simply because the hydrogen permeation tests are time consuming, expensive, and hydrogen concentration cannot be controlled. In addition, electrocharging method without coating of a catalytic layer on the membrane is appropriate to directly investigate the sole effect of hydrogen on the structural change of amorphous membrane. Therefore, even if the driving force for electrochemical hydrogen charging, that is, differential electrochemical

* Corresponding author. Tel.: +82 2 958 5456; fax: +82 2 958 5449.
E-mail address: efleury@kist.re.kr (E. Fleury).

potential of hydrogen ions in solutions on both sides of the membrane, is different from the driving force in real hydrogen permeation system, i.e., applied mechanical stress, the electrocharging method is preferred in order to directly insert hydrogen atoms into thin membrane. Like the experimental electrocharging method, hydrogen atoms are randomly positioned in the model sample, if the space between atoms is larger than the diameter of hydrogen atom. The amount of inserted hydrogen atoms (H/M) was varied from 2.5 to 100%, when comparing to the number of initial Ni and Al atoms (32,000). The hydrogenated samples were relaxed at 300 K below glass transition temperature, T_g (~500 K) for 100 ps, by applying NPT ensemble, because the experimental hydrogen permeation is usually performed at a temperature high enough to reach high values of diffusion rate.

To investigate the structure of the as-cast sample obtained by high cooling rate and structural change resulting from hydrogen charging, weighted Voronoi tessellation technique [17] which considers the effect of atomic size and classifies the 3D atomic configuration between the centered and the surrounding atoms, was used. The well-known, Voronoi tessellation technique is frequently used to probe them in the studies on amorphous materials using molecular dynamics [18]. It enables to precisely analyze their macroscopic behavior from the knowledge of their local atomic structures.

3. Results and discussion

The short-range ordered (SRO) structure of the prepared amorphous model sample was examined by calculating the fraction of Voronoi polyhedra using Voronoi tessellation method. Prior to the structural analysis, in order to compare the structure of this as-cast sample with one of the hydrogenated samples later, the as-cast sample was annealed at 300 K for 100 ps, which is identical to that of the hydrogenation condition. Although the metallic glasses consist of various short-range ordered structure more than 100 types indicated by Richards's indexing way [19], only the 19 representative Voronoi SRO structures were shown in Fig. 1. The $Ni_{90}Al_{10}$ amorphous model sample consists of various fractions of Voronoi polyhedra. Especially, the icosahedron indexed by (0,0,12,0) has the maximum fraction in amorphous sample. It is known that icosahedron has 5-fold symmetry that prevents long-range ordering, while it exhibits the densest packing, lowest potential energy together with the highest shear resistance [20].

Fig. 2 shows the spatial distributions of atoms in the as-prepared and hydrogenated samples as a function of hydrogenated fraction. Here, small red atoms are hydrogen atoms and they are randomly distributed in the whole sample. From a critical value of hydrogen concentration (around H/M = 30%), they agglomerate together and finally form hydrogen molecules by making nanovoids. The formation of nanovoids by hydrogen charging is considered to be
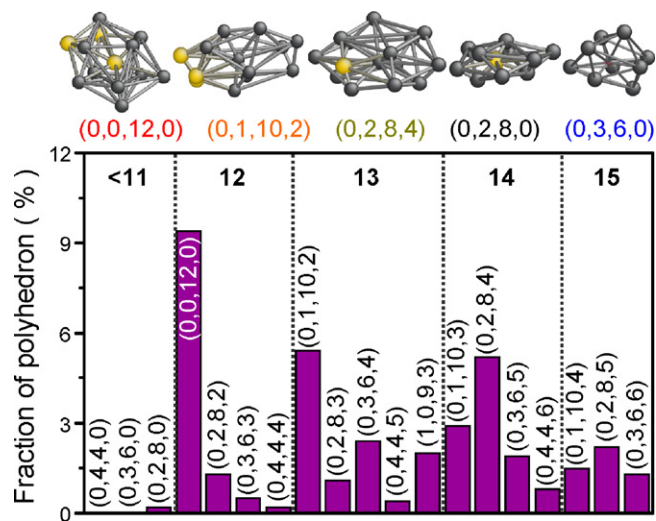
possible because experimental electrocharging for a long period induced the increase in the roughness and the formation of micro-crack on the surface of membrane [21]. This phenomenon might be originated from a dilatation of the amorphous structures by the hydrogen introduction. In detail, volume expansion in the hydrogenated sample was about 2.54% in H/M = 10%, 6.97% in H/M = 30%, 12% in H/M = 50%, which is in agreement with experimental observations [22].

A better understanding of the structural change of amorphous membrane due to the hydrogen insertion and a study clarifying the reason why that variation should occur, are necessary in order to find the fundamental strategy to enhance the hydrogen permeation properties. Therefore, the change in the fractions of several Voronoi polyhedra by hydrogen charging was investigated and was shown in Fig. 3(a). It was found that the fraction of icosahedron decreases with increasing hydrogen content, its decreasing rate becomes fast and then was followed by the saturation. Further, distorted icosahedral SRO structures, (0,1,10,2), (0,2,8,4), annihilated and finally saturated. In contrast, the relatively loosely packed (0,3,6,4) SRO structure collapsed at the initial stage of hydrogen charging (until H/M = ~10%) and then it was created slightly again for further hydrogen charging. Interestingly, prism and prism-like structures [23,24] with low coordination number, such as (0,3,6,0), (0,4,4,0), (0,2,8,0), were generated until H/M = 30%, and decreased slightly. Considering that the fraction of icosahedral structures is closely related to the degree of ordering in the SRO structures, such that higher fraction of icosahedron means higher degree of ordering [25,26], this result suggests that the structure of amorphous membrane becomes more disordered by hydrogenation. The evidence of this structural disordering upon hydrogen insertion was observed from the experimental data such as spot disappearance in the Fast Fourier Transform (FFT) image in HRTEM analysis [27], intensity decrease in the XRD [28], EXAFS analysis [28,29].

To trace the change in the configuration of representative SRO structures by hydrogen insertion, the variation of the fraction of X-centered (X = Ni, Al, H) polyhedra and X-neighbored (X = Ni, Al, H) polyhedra were examined. Among them, the change in the fraction of X-centered (0,3,6,0) polyhedron as an example of low index polyhedra was shown in Fig. 4(a), and the variation of (0,0,12,0) as an example of main amorphous SRO structures is displayed in Fig. 4(b). The fractional change of the H-centered of (0,3,6,0) is essentially characterized by the whole evolution of (0,3,6,0) SRO structure, while few Ni- or Al-centered (0,3,6,0) exist. This shows that the preferred central position to be occupied by hydrogen atoms are those in (0,3,6,0) clusters. But, from the continuous decrease in the number of Ni-, Al-centered (0,0,12,0) with increasing hydrogen content, the annihilation of (0,0,12,0) could be conjectured to stem from the collapse of all Ni-, Al-centered (0,0,12,0). Moreover, H-centered could hardly be found in (0,0,12,0). This result gives an evidence that (0,0,12,0) does not have an ability to lodge hydrogen atoms. From the investigation of the change of the composition within the neighboring sites of icosahedra, it was observed that its initial average composition maintains without large change, which supports well that the densely packed icosahedron has low ability to contain hydrogen atoms.

Further, to find the answer for the question how the initially existing amorphous structure of model sample is topologically altered by the hydrogen introduction, the structure of the hydrogenated samples was analyzed again by excluding hydrogen atoms from the sample used for Fig. 3(a) (Fig. 3(b)). From the Fig. 3(b), it was found that the structural change of main amorphous SRO structures have similar tendency to one in the sample included hydrogen atoms. Interestingly, the creation of (0,3,6,4) polyhedron was noticeable from H/M = 10%, which suggests that the initial amorphous structures become considerably looser than before. However, the prism and prism-like structures with low coordina-
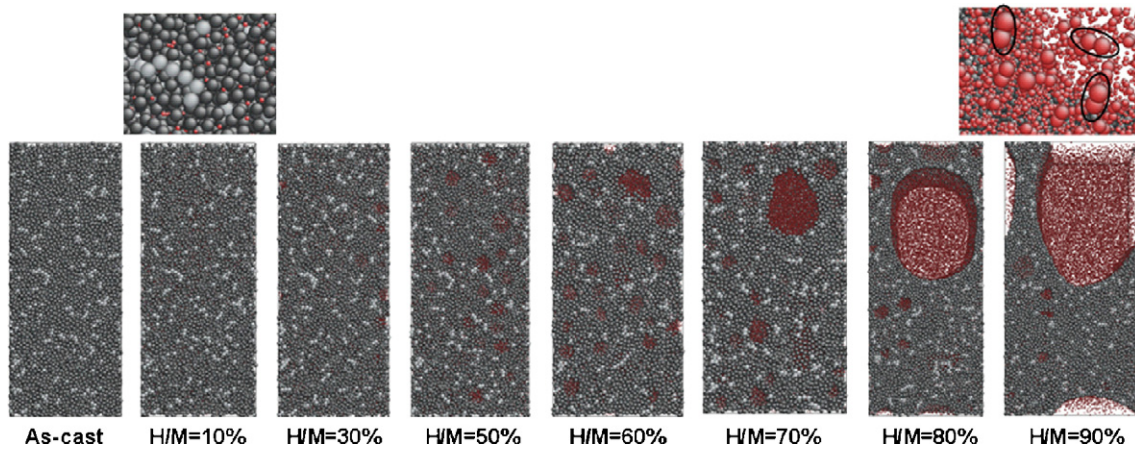

Fig. 1. Fractions of Voronoi polyhedra comprising the as-prepared amorphous sample. The Voronoi polyhedra were classified according to coordination number of polyhedra which are expressed on the top of the graph. The representative polyhedra, (0,0,12,0), (0,1,10,2), (0,2,8,4), (0,2,8,0), (0,3,6,0), are shown.

Fig. 2. Spatial distribution of hydrogen atoms in the amorphous samples as a function of hydrogen concentration.

tion number such as (0,3,6,0), (0,4,4,0), (0,2,8,0) were not detected in the sample excluding hydrogen atoms. This is because these prism-like structures are easier to accommodate hydrogen atoms and are directly related to the H-centered polyhedra with respect to the chemical composition.

The generation of prism-like structures is considered to result from the reconfiguration of nearest neighbor atoms around hydrogen atoms which are located in the relatively open space such as free volume. This is because hydrogen atoms are small enough to fill the open site, the generation of polyhedra with index of low coordination number such as (0,3,6,0), (0,4,4,0), (0,2,8,0) is possible. In addition, Ni or Al atoms around hydrogen atoms, that

is, Ni or Al atoms located in the neighboring sites of (0,3,6,0), (0,4,4,0), (0,2,8,0), find their stable sites, during which the newly formed polyhedra will induce the distortion of initial amorphous structures. Therefore, the existing icosahedral SRO structures annihilate. Further hydrogen insertion makes hydrogen atoms occupy positions not only in the sites with relatively open space which is the center, but also within neighboring sites of prism-like SRO structures (data was not shown here). This change of the configuration of prism-like structures could affect the configuration of icosahedral SRO structures which are connected to the prism-like structures and are sharing the neighboring atoms. Due to large atomic size difference between constituting atoms (Ni (1.246 Å) and Al (1.432 Å)) and hydrogen (0.37 Å), even at the insertion of one or two hydrogen atoms, the configuration of icosahedral SRO structures can be altered and finally they annihilate. Finally, polyhedra of low coordination number are reduced due to the formation of hydrogen molecules (from H/M = ~20%). This formation of hydrogen molecules is originated from the strong bonding of a hydrogen molecule between hydrogen atoms within prism and
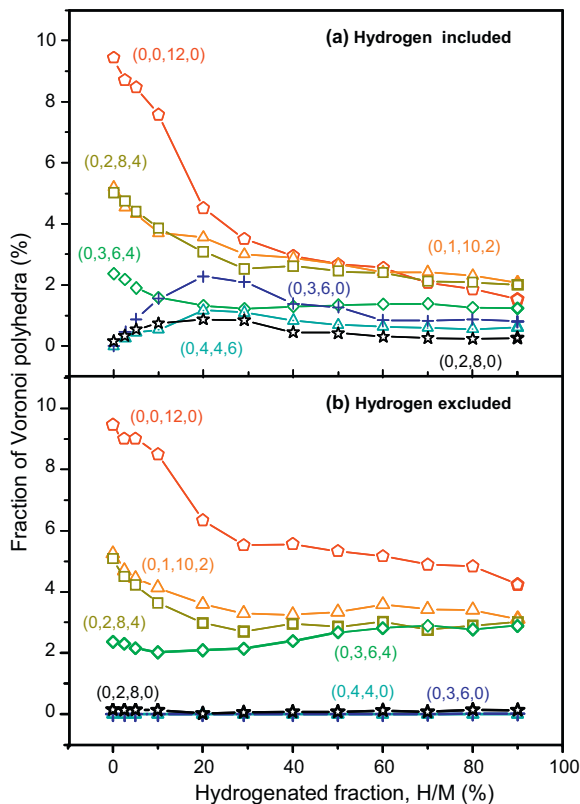

Fig. 3. Change in the fraction of representative polyhedra in the amorphous sample (a) included hydrogen and (b) excluded hydrogen as a function of hydrogen concentration.
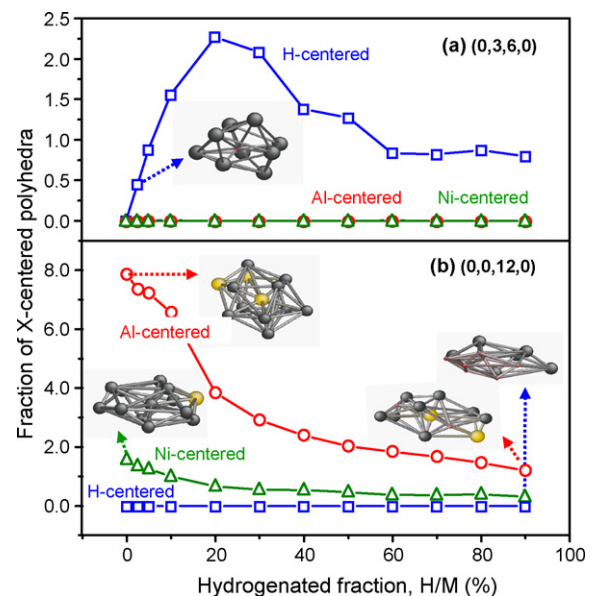

Fig. 4. Variation in the fraction of X-centered (X = Ni, Al, H) polyhedra. (a) (0,3,6,0), (b) (0,0,12,0) in the as-cast and hydrogenated samples as a function of hydrogen concentration.
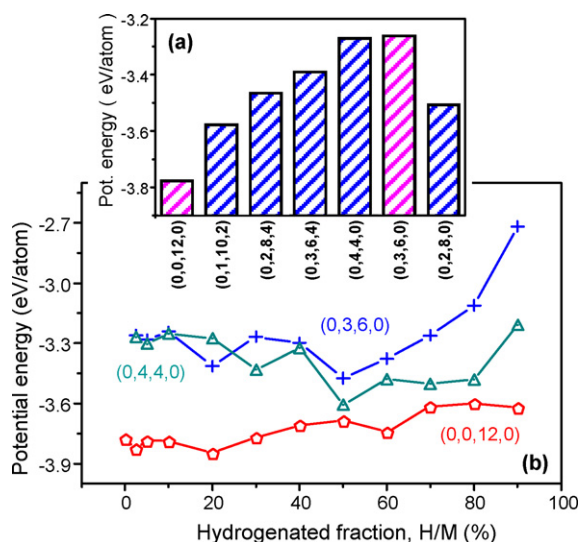
Fig. 5. (a) Average potential energy of representative polyhedra and (b) the variation of average potential energy of (0,3,6,0), (0,4,4,0) and (0,0,12,0) with respect to hydrogenated fraction.

prism-like structures or atoms near them, of which the H–H bonding could be energetically more stable than that of the isolated H atoms.

The generation and annihilation of various polyhedra are related to the stability of each polyhedron which is affected by the chemical composition or atomic configuration of polyhedron. The chemical composition and atomic configuration in various polyhedra determine their average potential energy. Therefore, to answer the question: why does the SRO structural change occurs during hydrogen insertion? the average potential energy of representative polyhedra in the hydrogenated sample (H/M = 2.5%) was calculated as shown in Fig. 5(a). Among several polyhedra, the average value of the potential energy is the minimum for icosahedron, while (0,3,6,0) has the maximum value, which suggests that as the hydrogen concentration increases, the initially stable icosahedra become unstable and annihilate. Meanwhile, (0,3,6,0) polyhedron was created since its energy was reduced, this SRO structure becomes finally unstable as further hydrogen atoms are inserted to form hydrogen molecules (Fig. 5(b)). From the point of structural stability view, it might be natural that small-sized hydrogen insertion into icosahedron which is most densely packed structure and has low ability to accommodate hydrogen, reduces the structural stability and finally icosahedral structures collapsed. On the other hand, (0,3,6,0) of low coordination number is easier to lodge small hydrogen atoms in both point of view, chemical composition and atomic configuration. Accordingly, the insertion of hydrogen atoms into prism-like structures makes that SRO structures more stable and the prism-like structure could be created until a critical value of hydrogen concentration. However, too much hydrogen charging brings about the increase in the structural instability of prism-like structures, which results in the formation of hydrogen molecules rather than being as isolated hydrogen atoms.

4. Conclusions

In summary, the hydrogen insertion into amorphous membrane induces structural changes by expanding the volume of membrane. In details, the initially stable and densely packed icosahedral SRO structures which have low ability to accommodate hydrogen atoms collapsed by becoming unstable, while the structures like (0,3,6,0), (0,4,4,0) with high affinity with hydrogen and high potential energy were created. This generation is closely related to the decreased potential energy with respect to hydrogen concentration.

Acknowledgements

References

[1] Y. Shimpoa, S. Yamaura, M. Nishida, H. Kimura, A. Inoue, J. Membr. Sci. 286 (2006) 170–173.
[2] S. Hara, K. Sakaki, N. Itoh, H.M. Kimura, K. Asami, A. Inoue, J. Membr. Sci. 164 (2000) 289–294.
[3] S. Yamaura, A. Inoue, J. Membr. Sci. 349 (2010) 138.
[4] S. Yamaura, M. Yokoyama, H. Kimura, A. Inoue, Int. J. Nucl. Hydrogen Prod. Appl. 2 (2009) 69–77.
[5] S. Yamaura, Y. Shimpo, H. Okouchi, M. Nishida, O. Kajita, A. Inoue, Mater. Trans. 45 (2004) 330–333.
[6] S. Yamaura, M. Sakurai, M. Hasegawa, K. Wakoh, Y. Shimpo, M. Nishida, H. Kimura, E. Matsubara, A. Inoue, Acta Mater. 53 (2005) 3703–3711.
[7] S. Hara, N. Hatakeyama, N. Itoh, H.M. Kimura, A. Inoue, Desalination 144 (2002) 115–120.
[8] K.B. Kim, K.D. Kim, D.Y. Lee, Y.C. Kim, E. Fleury, D.H. Kim, Mater. Sci. Eng. A 449–451 (2007) 934–936.
[9] D.Y. Lee, E. Fleury, Metal Mater. Int. 14 (2008) 545–548.
[10] H. Sakaguchi, G. Adachi, J. Shiokawa, Bull. Chem. Soc. Jpn. 61 (1988) 521–524.
[11] Y. Sakamoto, K. Baba, W. Kurahashi, K. Takao, S. Takayama, J. Non-Cryst. Solids 61/62 (1984) 691–696.
[12] N. Itoh, W.C. Xu, S. Hara, H.M. Kimura, T. Masumoto, J. Membr. Sci. 139 (1998) 29–35.
[13] K. Aoki, A. Horata, T. Masumoto, Proc. 4th Int. Conf. on Rapidly Quenched Metals, 1981, p. 1649.
[14] S. Jayalakshmi, J.P. Ahn, K.B. Kim, E. Fleury, J. Mater. Res. 22 (2007) 428–436.
[15] J.E. Angelo, N.R. Moody, M.I. Baskes, Model. Simul. Mater. Sci. Eng. 3 (1995) 289–307.
[16] M.I. Baskes, X. Sha, J.E. Angelo, N.R. Moody, Model. Simul. Mater. Sci. Eng. 5 (1997) 651–652.
[17] J.Y. Park, Y. Shibutani, Intermetallics 15 (2007) 187–192.
[18] M. Shimono, H. Onodera, Mater. Sci. Eng. A 515 (2001) 304–306.
[19] F.M. Richards, J. Mol. Biol. 82 (1974) 1–14.
[20] M. Wakeda, Y. Shibutani, S. Ogata, J. Park, Intermetallics 15 (2007) 139–144.
[21] N. Eliaz, D. Eliezer, Adv. Perform. Mater. 6 (1999) 5–31.
[22] S. Jayalakshmi, E. Fleury, J. ASTM Int. 7 (2010) JAI102522.
[23] T. Takagi, T. Ohkubo, Y. Hirotu, B.S. Murty, K. Hono, D. Shindo, Appl. Phys. Lett. 79 (2001) 485–487.
[24] J. Saida, K. Itoh, S. Sato, M. Imafuku, T. Sanada, A. Inoue, J. Phys.: Condens. Matter. 21 (2009) 375104.
[25] Y.Q. Cheng, A.J. Cao, H.W. Sheng, E. Ma, Acta Mater. 56 (2008) 5263–5275.
[26] K.W. Park, C.M. Lee, M. Wakeda, Y. Shibutani, M.L. Falk, J.C. Lee, Acta Mater. 56 (2008) 5440–5450.
[27] S. Jayalakshmi, E. Fleury, D.Y. Lee, H.J. Chang, D.H. Kim, Philos. Mag. Lett. 88 (2008) 303–315.
[28] A. Sadoc, V.T. Huett, K.F. Kelton, J. Phys.: Condens. Matter. 17 (2005) 1481–1492.
[29] R. Zehringer, E.K. Hlil, M.H. Tuilier, P. Oelhafen, H.J. Güntherodt, J. Non-Cryst. Solids 117/118 (1990) 425–428.